

**Harmonized production practices  
for volume data,  
low level reflectivity  
and weather radar wind profile**

A. Huuskonen, M. Kurri and J. Koistinen  
Finnish Meteorological Institute

OPERA-3 Deliverable

OPERA\_2008\_06

16 October 2009

# Contents

<b>1</b>	<b>Introduction</b>	<b>4</b>
<b>2</b>	<b>Volume data</b>	<b>5</b>
2.1	Definitions . . . . .	5
2.2	The concept . . . . .	6
2.3	Time stamp of volume data . . . . .	7
2.4	Operational measurement schedules . . . . .	8
2.5	Frequency of volume data . . . . .	10
2.6	Non-meteorological echoes . . . . .	11
2.6.1	Classification of echoes . . . . .	11
2.6.2	Ground clutter . . . . .	11
2.7	Attenuation . . . . .	13
2.7.1	Attenuation due to hydrometeors . . . . .	13
2.7.2	Atmospheric attenuation . . . . .	15
2.7.3	Wet radome attenuation . . . . .	16
2.8	Blockage . . . . .	17
<b>3</b>	<b>Calibration and monitoring of pointing and power</b>	<b>17</b>
3.1	Antenna pointing . . . . .	17
3.2	The power . . . . .	19
<b>4</b>	<b>Velocity volume data and Weather Radar Wind Profile</b>	<b>20</b>
4.1	Measurement methodology for velocity data . . . . .	20
4.2	WRWP product . . . . .	22
4.2.1	Choice of angles . . . . .	22
4.2.2	Radial velocity corrections . . . . .	23
4.2.3	Ground clutter . . . . .	24

<i>OPERA_2008_06: Harmonized production practices</i>	3
4.2.4 Other non-meteorological echoes . . . . .	24
4.2.5 WRWP processing . . . . .	25
<b>5 Low level reflectivity</b>	<b>26</b>
5.1 General remarks . . . . .	26
5.2 Processing . . . . .	26
5.3 Non-meteorological echoes, refraction and attenuation . . . . .	29
5.4 Correction of the effects of vertical displacement of radar measurements from the ground level . . . . .	30
5.4.1 Introduction . . . . .	30
5.4.2 Limitations of gauge-radar adjustment techniques to estimate low level precipitation . . . . .	32
5.4.3 Derivation and quality control of vertical reflectivity profiles from volume data . . . . .	33
5.4.4 Integration in time and place and limitations . . . . .	35
5.5 Requirements on volume data . . . . .	37
<b>6 Note on the frequency band and on the use of dual-polarization</b>	<b>38</b>
6.1 Choice of the frequency band . . . . .	38
6.2 Dual polarization . . . . .	38
<b>7 Appendices</b>	<b>39</b>
<b>A Finite bandwidth loss and the effective pulse length</b>	<b>39</b>
<b>B Power loss caused by the Doppler filtering</b>	<b>41</b>
<b>References</b>	<b>43</b>

# 1 Introduction

This document is the output of the OPERA 3 Work Package 1.6a "Harmonized production practices". The document presents recommendations on producing radar data, with the aim of increasing the quality and the harmonization of the radar data produced within the OPERA community. The recommendations are not restricted to the present state-of-the-art of making radar measurements. Instead, we wish to provide a view on how radar measurements are carried out in near future. In this sense, this document is intended as a guideline for the OPERA members when developing their network and operations.

The development of the weather radar hardware and software has been fast during the last ten years, and these developments must have an influence on the recommendations we wish to present to the community. The most notable new features are the digital receiver, which is a standard solution for any new installation, and the dual-polarization method, which is increasingly common in new installations. These new feature will change the way we operate the radars. Another important factor is the increasing speed of the transmission links, and the increasing storage capacity.

Another influential factor is the new uses of the radar data. The radar wind data is now used in numerical modeling, and thus there is an increasing demand of radial velocities. Also, a notable trend is the increasing use of radar reflectivity data in the quantitative precipitation estimation. Even though we are dealing primarily with the production practices for the volume data, we have to think of the uses of the radar data. Only then we are able to produce volume data which allow products of the best possible quality to be made.

The document is based on the output of earlier OPERA projects, on WMO documents and other available sources. An important OPERA source is Divjak *et al.* (1999), "Radar Data Quality-Ensuring Procedures at European Weather Radar Stations". It is a detailed summary of "*the main radar data quality-ensuring procedures, implemented or planned to be used in the next few years at operational weather radar sites in Europe.*" Divjak *et al.* (1999) restricted the treatment to pulsed conventional and pulsed coherent-on-receive radars with axially symmetric antenna patterns and with analogue logarithmic and linear receivers, as they constituted the overwhelming majority of contemporary radars used operationally by European national meteorological services at the time. We will update the focus,

because of the move of the European national meteorological services towards Doppler-radars equipped with linear receivers. This document is focused, but not fully restricted, to such radars. We will also discuss how the move towards dual-polarization radars would change our conclusions.

Another OPERA source is Germann and Galli (2003), which is a compilation of the scan strategies used within OPERA, and gives recommendations for scan strategies for a number of applications. The requirements of the user communities are described in Pohjola and Gjertsen (2006) and Chèze *et al.* (2009).

A general source of recommendations on weather radars is the CIMO handbook (WMO, 2006). The final report of a Swiss research project (Joss *et al.*, 1998) is a thorough document of the production practices especially for the precipitation measurements. The document also contains an extensive list of references. Meischner (2003) contains several articles which discuss various aspects of the weather radar networking and operations.

## 2 Volume data

### 2.1 Definitions

The first level of data, the radar raw data, is on the time domain level. The radar raw data consists of the output samples of the receiver, the in phase samples  $I(t_i)$ , and the quadrature phase samples  $Q(t_i)$ , complemented by the synchronization, calibration, timing, antenna position and status information. The sum  $I^2 + Q^2$  is proportional to the echo power, and  $\arctan(I/Q)$  is proportional to the echo phase (Divjak *et al.*, 1999). In a dual-polarization radar the  $I$  and  $Q$  samples are recorded both for the horizontal and vertical polarizations.<sup>1</sup>

The second level of radar data is the volume data, which will be discussed in more detail below. The radar volume data is calculated from the radar raw data and consists of a set of parameters which are calculated from the radar raw data in the signal processor. For single polarization radar these include the echo power ( $T$ ), the echo power after removal some types of echoes i.e. by high-pass filtering ( $Z$ ), the radial velocity ( $V$ ), and the spectral width ( $W$ ).

---

<sup>1</sup>Radars equipped with a logarithmic receiver record a signal proportional to the logarithm of the power. Although a logarithmic receiver is still quite common within OPERA, the type of receive will be obsolete in ten years of time, and will not be considered here.

And finally, the third level of radar data consists of products. Volume data serve as a starting point for the calculation of various derived quantities, represented as three-, two-, or one-dimensional fields in cartesian co-ordinates  $(x, y, z)$  over various projection planes, and referred to as radar site products. These products are traditionally grouped into three groups: reflectivity, precipitation, and wind products. Reflectivity and wind products may contain scattering from all types of scatterers, whereas precipitation products must be based on scattering from hydrometeors only.

## 2.2 The concept

The concept of volume data is used to describe a collection of data which samples the half-sphere above the radar in azimuth and elevation so that the meteorological phenomena of interest are recorded in the data set. Typically a volume data set consists of a number of azimuth rotation scans at various elevations. Further, it is typical that the lowest elevation is close to horizontal. The highest elevation, and the number of elevations used, depends on the qualities of the radar hardware and software and on the intended use of the data. These scans are conventionally called as PPI's (Plan Position Indicator) and consists of a number of rays, which are defined as data recorded as a function of range and integrated over an azimuth range, typically  $1^\circ$ .

It is further assumed that all data are recorded during a time span during which the changes in the target are negligible, or bearable. It is clear that this cannot always be the case.

There is no need that the radar software supports the concept of volume data, or even requests the user to apply it. A volume may be collected from individually recorded PPI scans, or there may be a number of individual PPI scans, of which some are selected depending on the use of the radar data. However, the concept of volume data is convenient and helps us to describe the data.

We define volume data as a collection of radar data, recorded as a function of range for a span of azimuths and elevations. The scope of this definition is rather wide, and may include cases which are not usually regarded as volume data.

### 2.3 Time stamp of volume data

It is stated in OPERA (1999) that *"as a general principle the time stamp in the basic radar site data should reflect, as accurately as possible, the time that the data was recorded. If possible each individual elevation scan should be independently time stamped as this will allow users of the data to easily decide whether the radar site data is timely enough for whatever purpose they wish to use it."* As summarized in OPERA (1999) it has been common to only record the start time, and occasionally also the end time of scans, these sometimes being just the start or end time of the volume scan and not the individual elevation scans.

These practices are not sufficiently good to achieve the goal stated above. If the start and end time of each PPI are given, and the start azimuth is not known, the timing of any ray in the PPI is known only to the half of the duration of the PPI. If only the start times are given, the accuracy is even less, as the start time of one scan is not the same as the end time of the previous scan. It is clear that using only volume start and end times is no more sufficient for present day needs.

A complete solution is to give the time of each individual ray of each PPI in the volume scan separately to a fraction of a second. However, a simpler solution is also possible as the antenna rotates in azimuth in a constant speed on each PPI. It is sufficient to record the start and end times of each PPI, together with the azimuth pointing at the start of the PPI and the direction of the rotation. The end time of the PPI can be replaced with the duration of the PPI. This information is sufficient to calculate the time stamp of each individual ray with an accuracy sufficient for all meteorological uses of the radar data.

Hence we are ready to give recommendations on time stamps. The first one is more in line with the present day practices, and the second is appealing due to its simplicity.

**Recommendation on time stamps:** It is recommended that the timing information stored with the data is such that the time of each individual ray of a volume scan can be calculated to an accuracy of 1 second.

**Further recommendation on time stamps:** It is recommended that the start and end times of each ray of a volume scan are stored to an accuracy of 1 millisecond or better.

## 2.4 Operational measurement schedules

The scanning strategies collected in the OPERA database were used by Germann and Galli (2003) to review the scanning strategies used by OPERA members. They pointed out that it is virtually impossible to set up a standardized set of scanning parameters and that there is no best solution. They further noted that, *"the design of the scan strategy is also led by the user requirements. Optimum specifications and parameter settings depend on the type of applications, such as qualitative monitoring of all types of precipitation up to long ranges, best quantitative estimates of surface rainfall at short ranges, measurement of snowfall, monitoring of echo top, retrieval of wind profile, and estimate of wind fields from single- and multi-Doppler retrieval techniques. The optimum solution for each of these fields of applications may look quite different. An objective analysis of the pros and cons and a discussion of the priorities is necessary to find the best solution in a given context."*

Hence one has to build the operational measurement scheduler on the user needs taking into account the capability of the hardware and software. The most important use of radar data is the estimation of the surface rain rate, but the use of radar data for producing vertical and horizontal cuts, echo tops, weather radar wind profiles and vertical reflectivity profiles need to be considered when designing the scheduler. The use of radar measurements in the numerical modeling is increasing, which means that radial winds are needed in addition to wind profiles. These uses put additional constraints to the design.

The estimation of the surface rain rate (and low level reflectivity) requires that low elevation angles are included in the scheduler. It is beneficial to have the lowest angle as low as possible, so that the observations are made close to ground and the deduction of the surface rain rate suffers to the least possible extent on the inevitable altitude separation of the ground the scattering volume. On the other hand, increasing the lowest angle reduces the amount of the ground clutter and a compromise between the two is made. This depends on the local orography. A low elevation angle may also increase blocking, either partial or full, and thus a somewhat higher angle is better. Often the lowest angle is at  $0.5^\circ$ , which is one half of a typical beam width of radar antenna. Hence the lower edge of the beam is close to the ground. In winter conditions a somewhat lower angle is often used. A most interesting way of solving the above problem in a complex orography is to change the elevation angle as a function of azimuth so that the lowest beam is

Table 1: A series of scans performed during 5 minutes

Task	A	B	C	D	E
Elevations [°]	0.3	3	2	7	15
	1.5	5		11	25
		9			45
Scan Speed [°/s]	16	22	22	24	30
Dual PRF	None	None	None	4:3	4:3
High PRF [Hz]	570	570	570	900	1200
Low PRF [Hz]				600	900
Nyquist speed [m/s]	7.6	7.6	7.6	35.9	47.9

kept at a fixed altitude above the ground (at a selected distance).

The angles above the lowest elevation have a set of applications. The most common of these applications are:

- One angle slightly above the lowest one is used to estimate the reflectivity at points where the lowest angle is severely contaminated by ground clutter or suffers from beam blockage, either partial or complete
- horizontal cuts at various altitudes (CAPPI)
- vertical cuts of the radar reflectivity fields
- height of the echo top
- radial winds to produce wind profiles (WRWP)
- vertical reflectivity profile
- vertical integrated liquid (VIL)
- probability of hail

The number of these elevation angles varies a lot, but is mostly from 10 to 15. Increasing the number improves the quality of the products by making the interpolation simpler, but decreases the statistical accuracy at each point. The quality is increased by increasing the total time used to measure these angles, but then the changes in the reflectivity field are larger and the quality of the products suffers from that.

Table 1 shows an implementation of these planning principles to an operational scan scheduler, based on the practices used at FMI. During a 5 minute scan,

altogether 11 elevation angles are measured, which are grouped into 5 sub scans for clearer presentation. Task A is intended for precipitation products, while the other tasks are needed to produce the list of products detailed above.

The scheduler presented in Table could be repeated at 5 minute intervals. Another option is to change the angles, except some of the lowest ones, for the next 5 minute period. Then there are more angles to be used for horizontal and vertical cuts, albeit with a risk of reduced stationarity. Yet another option is to repeat some of the subtasks only, which is the case at FMI. Tasks A and B are repeated at every five minutes, but tasks C-E only at every 15 minutes. This gives room for other type of measurements, e.g. to measurements of radial winds at low elevations.

Finally, all this has to be rethought when we have a dual-polarization radar. A straightforward solution is to use both polarizations at every task. Then there is a 3 dB loss of sensitivity, which can be compensated by using a transmitter with a doubled peak power. Not all tasks, however, benefit of the dual-polarization, hence a more optimal solution is to use the dual-polarization for most sub tasks, but not necessarily for all. And finally, dual-polarization radars usually perform an azimuthal scan in zenith to calibrate  $Z_{dr}$ , which calibration measurement has no counterpart in single polarization. The frequency of such a measurement depends on the stability of the system. The experience on the planning of the schedulers for operational dual-polarization radars is still very limited. It is expected that such experience is emerging during the next few years.

## 2.5 Frequency of volume data

Volume data are usually produced at every 5, 10 or 15 minutes. In the latter two cases, the lowest angles are usually repeated at every 5 minutes. There is no self-evident choice to the frequency other than it is convenient to use a fraction of full hour. It is also convenient to use a fraction of half an hour or a quarter of an hour, also these guidelines are less stringent. With this the only viable option, except to using 5 minutes, is to use a 2.5 minute scan interval. We also may point out that some satellite data are produced at 5 minute intervals, and coordination with that data is also useful.

**Recommendation on the frequency of volume data:** It is recommended that volume data is produced at a time interval, which is an integer multiple of 5 minutes, or a fraction of 5 minutes.

It is important to note that not all repetitions of the scheduler need to be identical. There may be variations in the elevation angles, antenna speeds, pulse lengths etc. But the volume data produced during each repetition should be similar enough that the most important products can be produced at the stated frequency.

## 2.6 Non-meteorological echoes

### 2.6.1 Classification of echoes

As the main use of the radar volume data is to obtain precipitation products, a number of methods have been developed to detect and remove non-meteorological echoes from the data. An ongoing trend is to move towards a classification of echoes. Instead of simply removing the non-meteorological echoes, a probability distribution is given. The probability distributions can be seen as quality fields of the volume data, indicating how useful the data is for a given application. Peura (2002) presented a set of detectors for various non-meteorological targets and showed examples of their application. Some echo types can be classified by single polarization data, but the introduction of the dual-polarization has given new tools for the classification. The classification of echoes is closely related to the work on quality information (Holleman *et al.*, 2006).

The detection, classification and elimination of most of the non-meteorological echoes is based on studying the features of the parameter fields of the volume data. Hence there is no need to remove these echoes at the production stage. It would be advisable to provide quality fields which give the probability of each echo type, and provide the fields with the data. But as this might manyfold the data size, it may be better to leave the detection and elimination to the user.

There are some exceptions to this recommendation, most notably the ground clutter, which is discussed below separately.

### 2.6.2 Ground clutter

The ground clutter deserves a separate treatment, because the clutter signal is often strong, and many methods to deal with the clutter are implemented into

the volume data production. These methods cannot be applied any more to the radar volume data. The following methods are used:

1. High pass filtering, in which the  $I(t_i)$  and  $Q(t_i)$  are high pass filtered before the volume data is calculated
2. Removal of clutter signal using frequency domain methods
3. Oversampling methods, in which the second order moments are first calculated with a high radial resolution, bins affected by the clutter removed, and the moment estimates calculated using samples not affected by the clutter
4. Removal based on clutter maps, which may be static or dynamic

**High pass filtering** is a straightforward way to remove the ground clutter on a Doppler radar. Radar software packages contain a series of high pass filters with increasing stop band widths. The operator selects usually the narrowest filter which is wide enough to remove the clutter. The spectral width of the clutter signal depends on the source, but also on the stability of the radar transmitter and receiver systems. An unfortunate drawback of the high pass filtering is that some weather signal will also be filtered. Regions with radial velocity close to zero will get attenuated ("Doppler snake"), and there are indications that all weather signals are somewhat attenuated. The latter effect depends on the implementation of the filter, see Appendix B for further details.

A variant of this method is to use the high pass filtered data only to indicate where some ground clutter appears. In the further processing the difference between the unfiltered data (T) and filtered data (Z) is used as a quality factor.

**Frequency domain methods** are based on the fact that the clutter signal is at the zero frequency and that the spectral width of the clutter signal is much smaller than that of the weather signal. In the method some of the frequency bins around the zero frequency are interpolated using the adjacent spectral values and the original spectral data discarded. The method should, in principle, be more effective than the time domain high pass filtering, and should remove less weather signal. This method can, as the previous one, be used just to indicate where ground clutter appears.

**Oversampling methods** are based on calculating the data in the first stage at a much higher radial resolution than the resolution of the volume data to be stored. The clutter removal is based on studying the SNR, coherence, velocity and other properties of the signal, as well as on studying the distribution of the power within the set. Bins classified as clutter are rejected, and the estimate is made on averaging the remaining measurements. The method is outlined in Joss *et al.* (1998) and Germann and Joss (2003). The method can also use the information provided by the previous methods as an input. In a simplified model only the distribution of the power is studied, and bins with power deviating from the average are removed.

**A clutter map** is the only way to remove clutter with non-Doppler radars. With Doppler radars it may provide an additional stage after the more advanced methods have been used. The outcome of the clutter analysis should be used to update the clutter map during every scan. An adaptive clutter map is more efficient than a static map based on long term averages.

## 2.7 Attenuation

The radio waves on their way from the radar to the scattering volume and back are attenuated by the atmospheric gases and by the hydrometeors. These effects will be treated in this section, together with the attenuation on the surface of a wet radome.

### 2.7.1 Attenuation due to hydrometeors

The attenuation of the radio wave due to hydrometeors depends on the water phase and on the total amount of water in the volume. At the S-band the effect is minimal and can safely be neglected. At the C-band the effect is significant, but is mostly neglected due to problems in estimating the attenuation. The following formulas for the one-way attenuation  $a$  are valid for the S-band and the C-band, respectively (WMO, 2006):

$$\begin{aligned} a &= 0.000343R^{0.97} \\ a &= 0.0018R^{1.05} \end{aligned} \tag{1}$$

where  $R$  is the rain rate in units  $\text{mmh}^{-1}$ . The equations reveal the first problem of the attenuation correction. The attenuation depends on the total water content

Table 2: The calculated attenuation in dB for rain rates and calibration errors given in the table. The attenuation is calculated for a total distance of 100 km. The true attenuation is seen on the line for the 0 dB calibration error.

Calibration error [dB]	Rain rate [mm h <sup>-1</sup> ]					
	1	2	4	8	16	32
-5	0.2	0.3	0.7	1.3	2.3	3.5
-4	0.2	0.4	0.8	1.6	2.8	4.3
-3	0.2	0.5	0.9	1.8	3.4	5.4
-2	0.3	0.5	1.1	2.2	4.2	6.9
-1	0.3	0.6	1.3	2.6	5.2	9.2
0	0.4	0.7	1.5	3.2	6.6	13.5
1	0.4	0.9	1.8	3.9	8.7	66.8
2	0.5	1	2.2	4.8	12.5	Inf
3	0.6	1.2	2.6	6.1	26.3	Inf
4	0.7	1.4	3.2	7.9	Inf	Inf
5	0.8	1.7	3.9	11	Inf	Inf

and not on the reflectivity, measured by the radar. Hence a Z-R relationship needs to be used to estimate the attenuation. Also, a miscalibration of the radar has its effect. If the reflectivity is overestimated, the attenuation correction will be overestimated as well, resulting in a rapid increase of the error in the correction with the range. This is demonstrated in Table 2, which gives the error in the estimated attenuation for a set of rain rates and radar miscalibration factors. A Z-R relationship

$$Z = 200R^{1.6} \quad (2)$$

is used. The table shows that up to a miscalibration factor of 2 dB the error caused by the miscalibration is smaller than the attenuation up to the rain rate of 16 mmh<sup>-1</sup>. We may conclude that in these cases the attenuation correction even with miscalibration produces a smaller error than neglecting the attenuation correction totally. However, with larger calibration errors and rain rates the error in the calculated attenuation increases rapidly.

There are, however, a number of additional error sources which have to be taken into account

- Large reflectivity values are often caused by the hail, which does not attenuate a lot. If the hail is not detected, the attenuation is overestimated.

- The attenuation depends on the water phase, which is not obtained from (single polarization) data. Synoptic observations and model fields can be used to produce 3-D water phase models to take this into account.
- The attenuation in the sleet is still largely unknown.
- Moving targets, e.g. ships, produce high reflectivity values and cause artificial attenuation

It is evident that neglecting the attenuation results in a systematic underestimation of the radar reflectivity at longer ranges. Reliable estimation of the attenuation is difficult, because of the many error sources present. With the increasing efficiency of the classification of the data, and increasing capabilities to determine the water phase, the prospects of doing reliable attenuation estimation increases. It is clear that reliable estimation of the rain rates is not possible without taking attenuation into account.

Dual-polarization measurements provide additional data, which are proportional to the attenuation. An evaluation of correction methods is presented in the report of the OPERA 3 Work Package 1.4 (Tabary *et al.*, 2009).

**Recommendation on attenuation correction:** We recommend that no attenuation correction due to hydrometeors is done to the radar volume data but that the attenuation is taken into account when products are calculated.

The above recommendation is equally valid for single and dual polarization data. However, due to restrictions in the storage space or the transmission line capacity, the dual polarization moments needed for the attenuation correction may not be saved with the volume data. Then the rain attenuation correction has to be done to the volume data, or otherwise the possibility for the correction is lost.

### 2.7.2 Atmospheric attenuation

All radio waves are attenuated when they are traversing the atmosphere due to interaction with the neutral atmosphere. The attenuation depends on the density of the atmosphere, but it is a standard procedure to neglect the decrease of the density with altitude and to apply a single attenuation constant. A standard value for the one-way attenuation constant is  $0.008 \text{ dB km}^{-1}$ . Thus at a distance of 250 km the total two-way attenuation amounts to 4 dB.

**Recommendation on atmospheric attenuation:** We recommend that the correction due to atmospheric attenuation is done to the radar volume data.

### 2.7.3 Wet radome attenuation

Water on the surface of a radome attenuates radio waves. The amount of water depends on the rain rate, and on the properties of the radome surface. Also the wind speed and direction have their effect on the distribution of water on the surface, and hence on the attenuation. And finally, the water phase is significant as well.

The case is very complicated, and at present there is no model to calculate the attenuation due to water on the radome surface at a function rain rate, wind speed and direction, taking into account the radome properties. Laboratory measurements and model calculations in the absence of wind give insight into amount of attenuation. At  $10 \text{ mmh}^{-1}$  the one-way attenuation of an old radome is about 1 dB, and at  $15 \text{ mmh}^{-1}$  about 1.5 dB, including the dry radome attenuation of 0.35 dB. The two-way attenuation is then over 2 dB, which is significant (Kurri and Huuskonen, 2008; Manz *et al.*, 1999).

However, the properties of the radome surface determine to a large extent in which form the water runs down along the surface. There may be a water film, the water may exist as droplets, or run down as rivulets. The same amount of water on the surface, but with different form, produces a different amount of attenuation, the attenuation being smaller when the water remains as droplets on the surface of the radome. A hydrophobic treatment of the radome is an effective way to decrease the attenuation. Firstly, the water stays better as droplets and, secondly, the water runs down along the radome faster. Therefore the uncertainty is best minimized by using radomes with suitable coating.

Wet snow or undercooled water may attach to the radome surface, which may even completely block a sector in the data. This is best attacked by applying heating inside the radome.

**Recommendation on radome:** It is recommended that the effect of the wet radome attenuation is minimized by a suitable coating on the radome surface and the accumulation of snow and ice is attacked by heating the radome.

## 2.8 Blockage

The siting of a radar is most important for the quality of the measurements. In an ideal case, a radar should be situated so that the horizon is at all directions below  $0^\circ$  elevation, and that there are no masts, buildings or other obstacles in the surroundings. This is very rare in real life situations.

In a flat terrain the above can be accomplished in most cases by raising the antenna high enough by means of a high tower. But even then obstacles, such as antenna masts and wind turbines, may extend above the horizon. In a hilly or mountainous terrain the raising horizon inevitably produces blockages, except when a radar is sited at the top of the highest mountain.

The blockage can either be partial or total. In the latter case the radar beam does not extend beyond the obstacle causing the blockages, whereas in the former case only part of the beam is blocked.

The blocking cases which are caused by masts and towers and other extended objects and which do not cause a total blocking in the azimuth, are the easiest ones to handle. In such cases it is possible to calculate the percentage the angular distance blocked and to use the result to correct the data. Another possible way to estimate the correction is to use long time rain accumulations. Based on this, a correction factor is estimated and applied to correct the data.

A similar approach is possible for partial blockage caused by raising horizon, although in this case the blockage varies with the weather, as the propagation paths are changing. If the blockage is total, no correction method is available, and it is necessary to use data from higher elevations. It is also possible to change the elevation angle as a function of azimuth so that the lowest beam is kept at a fixed altitude above the ground (at a selected distance).

## 3 Calibration and monitoring of pointing and power

### 3.1 Antenna pointing

The antenna pointing needs to be monitored, especially in the elevation. The WMO CIMO handbook (WMO, 2006) states that the elevation and azimuth angles shall be accurate to  $0.1^\circ$ . In practice the need for accurate pointing is more

evident in the elevation than in the azimuth, because an error at low elevations changes the altitude of the scattering volume significantly, whereas a corresponding error in azimuth has less severe consequences. However, the given accuracy is achievable in both. We describe below some methods which are used for checking the antenna pointing, and discuss how it is possible to monitor the pointing on-line.

The checking of the antenna pointing in azimuth is quite straightforward. Fixed objects such as masts are used, as well as observations of the sun. With these methods the antenna is aligned easily to the required accuracy.

For elevation, two types of methods are used. The first is based on measuring the orientation of the antenna dish, and the second on measuring the direction of the electro-magnetic beam of the antenna.

The orientation of the antenna dish is measured by the plumb line method. The antenna is positioned at a small negative elevation, e.g.  $-1^\circ$ , and the distance of plumb line, attached to the upper edge of the antenna dish, and the lower edge of the antenna dish is measured. The true elevation pointing of the antenna is obtained by simple trigonometry. It is necessary to ascertain that the antenna base itself is upright. This is done by repeating the plumb line measurement at several azimuthal pointings. The difference of the readings tells how much the antenna base is tilted.

These measurements are simple and are easy to do during the maintenance. The weak point, of course, is that the result tells only the orientation of the antenna dish, but not that of the electro-magnetic beam, which we wish to determine. Any misalignment of the antenna feed is directly seen as a difference of the mechanical pointing and the electro-magnetic pointing.

The sun is the best choice for checking the the electro-magnetic pointing of the antenna system. The standard method is to observe the sun direction close to noon, when the sun elevation changes only slowly with time. Both manual and automated methods are available. Both give the antenna offset in the elevation and also in the azimuth. An accuracy better than  $0.1^\circ$  is obtainable. The measurements are mostly done during the maintenance, but tools which can be run from the operational scheduler are also available. In that case the offset check can be done even daily.

The sun observations close to noon are done at quite high elevations. At the  $50^\circ$

latitude the elevation is  $17^\circ$  at the winter solstice and  $63^\circ$  at the summer solstice, whereas the most important scans for precipitation products are done at low elevations. In case the antenna elevation scale is not linear, a match to the sun at an high elevation does not prove that the elevation of the low elevation scans is correct. This problem is circumvented if the sun is observed at elevations close to the horizon. Automated methods have to be used because the sun elevation is changing rapidly. Such tools are contained in the radar software tools for off-line checking. Huuskonen and Holleman (2007) present a method to determine the antenna azimuth and elevation from operational scan data.

**Recommendation on monitoring the antenna pointing:** It is recommended that radar system is equipped with automated tools which determine the antenna pointing at regular intervals.

## 3.2 The power

The received power  $P(r)$  and the reflectivity  $\eta$  are connected by the radar equation (Doviak and Zrnić, 1993, chap. 4.4.1):

$$P(r) = \frac{P_t g^2 g_s \lambda^2 c \tau \pi \theta^2}{(4\pi)^3 r^2 l^2 l_r 16 \log 2} \eta. \quad (3)$$

A good knowledge of the various factors appearing in the equation is essential to measure the reflectivity properly. The sources for these factors vary:

- The antenna gain  $g$  and the antenna 3 dB beam width  $\theta$  are provided by the antenna manufacturer
- The wave length  $\lambda$  depends on the transmitter operating frequency
- The pulse length  $\tau$  is measured during the calibration
- The transmitter power  $P_t$  is measured during the calibration and, preferably, monitored during the radar operation. The peak power should be determined from the averaged transmitter power, because the product  $P_t \tau$ , which is proportional to the average power, appears in the radar equation.
- $l$  is the loss caused by the atmosphere and hydrometeors, which has been discussed in section 2.7
- $l_r$  is the loss due to finite bandwidth of the receiver, which is described in Appendix A

- $g_s$  is the system power gain, which is taken care of by the calibration
- $r$  is the range to the scattering volume,

In addition, there are a number of factors, which do not appear in the radar equation as presented here. These factors include the transmitter losses from the power measurement point to the antenna feed, the dry radome loss, and the receiver losses from the antenna feed to the calibration injection point. These factors are taken care of in the calibration, or they are applied when calculating the received power.

Monitoring operationally the complete transmitter-receiver chain is demanding, because it requires target with known scattering properties. Such targets are not readily available. However, returns from mountains or other similar objects have been used to monitor the stability of the chain.

For the receiver chain many more possible methods exist:

- The radar receiver can have a reference noise source. The injected noise is measured and used as a reference.
- The radar can measure the sky noise at high elevation, and use it as a reference.
- Solar radiation can be used to monitor the receiver stability (Holleman *et al.*, 2009)

## 4 Velocity volume data and Weather Radar Wind Profile

### 4.1 Measurement methodology for velocity data

The main use of the weather radar data is in precipitation products, and wind products are often only a side product. In case the precipitation and wind products have contradicting requirements, those of the precipitation products dominate, due the bigger importance of the precipitation. As the so-called range-velocity ambiguity limits our free choice of maximum range and velocity to be measured, we thus usually limit the velocity range. Figure 1 shows the Nyquist velocity, i.e. that highest velocity measurable when the measurement is restricted

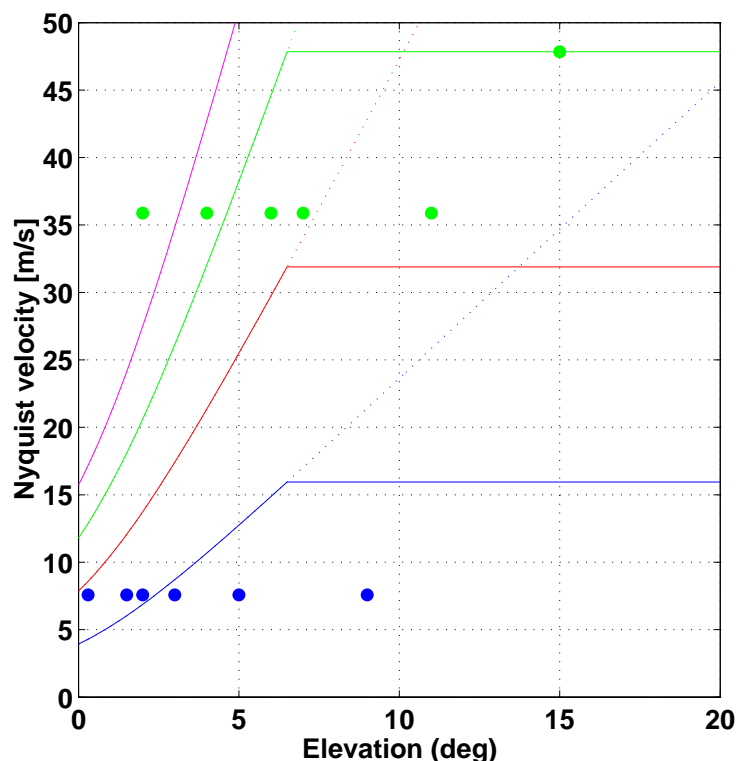


Figure 1: The Nyquist velocity calculated for a single PRF (blue) and a dual PRF of ratios 2:3 (red), 3:4 (green) and 4:5 (magenta), assuming the PRF chosen so that the range is covered until the height of 15 km is reached (solid and dotted curved lines). The effect of the maximum available PRF of 1200 Hz is denoted by the horizontal lines. The elevation angles and Nyquist velocities of the FMI radar tasks are denoted by filled circles. Their colour is as above.

by the range-velocity ambiguity, as a function of the elevation angle<sup>2</sup>. We assume that the highest altitude to be measured is 15 km, and that we select the Pulse Repetition Frequency (PRF) so that no second trip echoes are observed. Thus a point below/right of a line represent measurements which have no risk of second trip echoes. Points above/left of a line face the risk. Yet velocity data is often recorded with such measurements, because the random phase nature of the magnetron transmitter transforms the second trip echoes to an additional noise component, when velocity data is only considered. As an example, the elevation/Nyquist velocity values for the operational FMI measurements are shown in the figure.

<sup>2</sup>The majority of Doppler-radars within OPERA are C-band radars. In fact, there are 125 C-band Doppler radars, and only 11 S-band Doppler radars. These numbers are based on entries at the OPERA database on 1 September 2009. Therefore we restrict the discussion on velocity volume data and Weather Radar Wind Profiles (WRWP) to C-band.

For a single PRF measurement (blue line) the maximum velocity ranges from 4  $\text{ms}^{-1}$  upwards. The velocity increases with an increasing elevation, because the maximum range decreases and the PRF can be increased. At some elevation we hit the limits of the transmitter. The figure assumes that 1200 Hz is the highest PRF which can be used. We hence note that the maximum velocity is at most about 16  $\text{ms}^{-1}$ .

It is clear that this is not sufficient. Radial velocities at least up to 30  $\text{ms}^{-1}$  must be measured and even higher velocities at times. We note that a dual PRF with ratio 2:3 would increase the maximum to 32  $\text{ms}^{-1}$ , and a ratio 3:4 to 48  $\text{ms}^{-1}$ , which is sufficient for most occasions. If we place the velocity limit to 40  $\text{ms}^{-1}$  we see from Fig. 1 that for elevations above about 5° we can use the same measurement for the velocity and reflectivity observations, assuming a ratio of 3:4. The elevation limit depend on the assumptions. The limit given is rather conservative and there are grounds to use a lower elevation limit. A velocity limit of 30  $\text{ms}^{-1}$  and highest altitude of 12 km would result in an elevation limit of 3°.

## 4.2 WRWP product

The discussion on the production practices of weather radar wind profiles is based on Holleman (2003), Holleman and Beekhuis (2003), and Holleman (2005). These papers contain material on the phenomena which affect the quality of the WRWP, and which are discussed below.

### 4.2.1 Choice of angles

The elevation angles in which the radial velocities need to be measured depend on the altitude range of the WRWP and also on the horizontal homogeneity assumed. The WRWP estimate is based on radial velocities from a cylinder (VVP processing) with an inner and outer diameter. Figure 2 shows the altitude of the center point of the beam as a function of the elevation angle and the distance from the radar. Assuming that altitudes up to 6 km are wanted and that data between 10 and 30 km from the radar are used, elevations at least up to 11° are needed. A lower limit of 0.5 km would mean that radial velocities are needed down to elevations of 3°.

As Holleman (2003) points out one should avoid so high elevations that the fall speed of the hydrometeors has a significant effect on the radial velocity. The

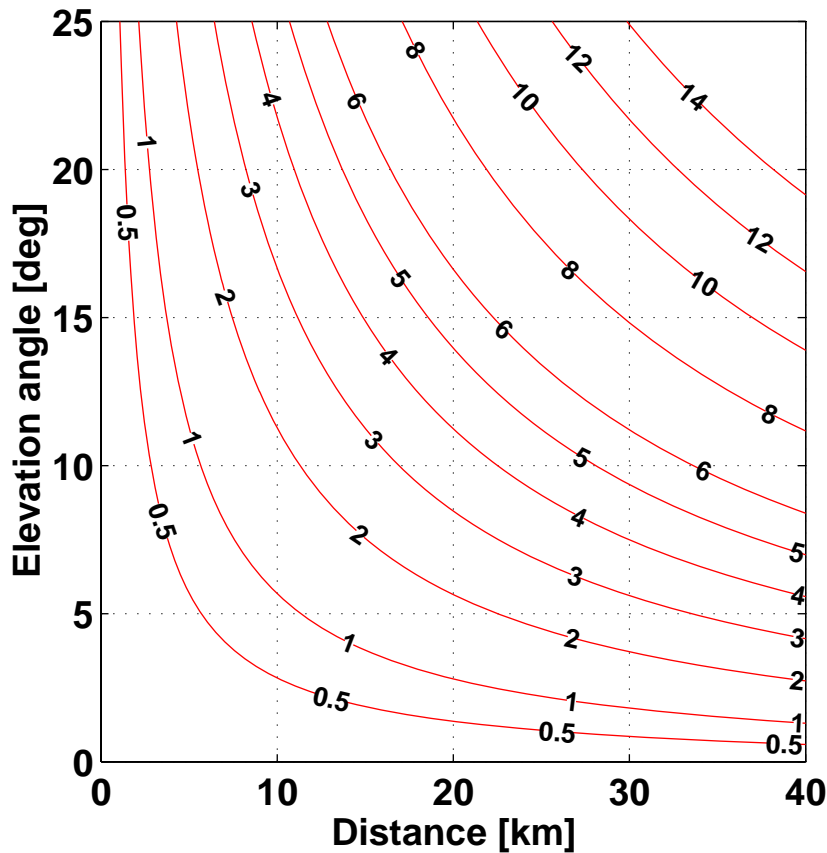


Figure 2: The height of the radar beam as a function of the distance from the radar and the elevation angle for the 4/3 refraction model.

WRWP processing can estimate the vertical component of the velocity as well, but any inhomogeneity in the vertical velocity field will bias the horizontal velocity. Elevations above  $25^\circ$  are usually regarded as problematic in this respect.

#### 4.2.2 Radial velocity corrections

The dual-PRF algorithms always produce a certain number of wrong estimates, in which the radial velocity is in error by twice the Nyquist velocity of the lower or higher PRF used. These errors occur when the algorithm unfolds the velocity incorrectly. Holleman and Beekhuis (2003) report that some 1% of the radial velocities are wrong. These velocities decrease the quality of the WRWP. The following methods are available to handle these velocities and prevent them from decreasing the quality of the WRWP:

1. Analysis of the radial velocity field in the azimuth and radial directions to

- find out out-liers in the field and a subsequent correction.
2. Analysis as above, but the suspected out-liers are marked as bad data.
  3. Analysis of the radial velocity field after a first estimate of WRWP has been produced. The out-liers are either corrected or marked as bad data.

The most complete way is a combination of methods 1 and 3, although there may be problems in picking the incorrectly unfolded velocity points. Method 3 works well when the number of out-liers is low.

### 4.2.3 Ground clutter

The ground clutter biases radial velocity estimates towards zero. Even though the volume data is clutter filtered, bins remain with residual ground clutter, which is small enough not to affect the reflectivity fields, but significant enough to show in velocity fields. The bias is larger when the weather signal is weak. This is very well seen in Fig. 3, which shows statistics over one month for the FMI Vantaa radar. A large standard deviation is visible at all height below 2 km. During the summer months, when the weather signal typically is stronger, the bias is significantly smaller.

There are several ways to decrease the clutter effect by improving the processing:

1. Stronger filtering is performed to the velocity field. The clutter-to-signal ratio level is defined so that the weather echo is the dominant source for any velocity estimate used in the WRWP processing
2. All radial velocity values below a set limit are discarded. A limit of  $2 \text{ ms}^{-1}$  is recommended by Holleman (2005).

### 4.2.4 Other non-meteorological echoes

Any object which moves with its own velocity, and not with the wind, is a problem for the wind determination. These objects include ships, aeroplanes and birds. Holleman *et al.* (2008) have recently discussed the effect of bird migration on the quality of radar winds.

Insects, as well as dust in the atmosphere, are so light that they travel with the wind. They do not bias the velocity data and actually are useful as scatterers when there is no rain.

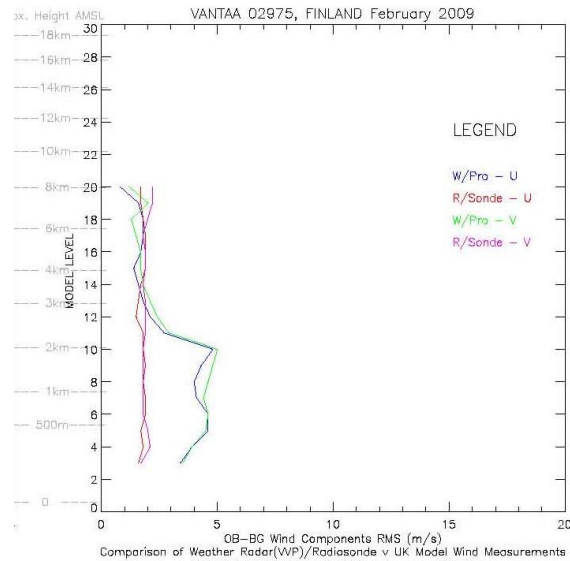


Figure 3: The standard deviation between the WRWP winds and the Met. Office model winds for the Vantaa radar in February 2009. The green and blue lines give the statistics for the radar wind components, and the red and magenta lines corresponding statistics for the winds from radio soundings of nearby stations.

#### 4.2.5 WRWP processing

Assessing WRWP processing algorithms is beyond the scope of this document. A good reference work is Holleman (2005). Whatever algorithms is used, it is important to process the data so that the problems related to the radial velocity and the ground clutter are taken into account. Other sources of error, e.g. birds, may be significant for certain radars and times of year as well.

A trade-off between the availability and the quality of the WRWP profiles has to be made. If the settings are such that the amount of profiles is emphasized, more lower quality profiles pass through the processing, and vice versa. However, it is not good to tighten the screening so much that good quality profiles are unnecessarily discarded. Recommended settings for some systems are given by Saltikoff and Holleman (2004).

**Recommendation on WRWP processing:** It is recommended that WRWP processing is done so that incorrectly unfolded radial velocity estimates do not contribute to WRWP and that estimates biased by ground clutter are not used.

## 5 Low level reflectivity

### 5.1 General remarks

The low level reflectivity is the base product which is the source for estimating precipitation at the ground and also to make reflectivity composites. The task of describing the production practices of the low level reflectivity in general is wide, because the methods to be used depend e.g. on the orography, and the network structure.

We will limit our discussion to describing a product which can be used to make European composites in the OPERA radar data center. This allows us to make some simplifying assumptions. First of all, most of the OPERA area is covered by a dense network of radars, as seen in Fig 4. Figure 5 shows that for some 30 % of radars the nearest radar is at an distance shorter than 100 km, and for 60 % of the radars the distance is less than 150 km. And the majority of the radars (90%) have an radar closer than at the 200 km distance. This analysis is not complete, because at any radar there are sectors where the nearest radar is further, and the radars at the edges of the network and close to the sea have sectors with no radar within their operational range. The two-dimensional distance distribution is portrayed in Fig. 6 which shows the distance to the closest radar. It is seen that most locations within the OPERA radar network are closer than 100 km from the nearest radar. Hence we can choose data processing methods which are good up to 100 km distance, but need not be optimal at longer distances.

The restriction to 100 km has also its implications on the compositing algorithms. We have to assume that the data at long ranges do not appear in composites. Otherwise the long range reflectivity data overcorrected by some algorithm might dominate the composite. This implies that the compositing algorithm must not be based on maximum compositing.

### 5.2 Processing

The low level reflectivity field is calculated from the volume data in a number of processing steps, which include the removal of non-meteorological echoes from the data, the attenuation correction, and the deduction of the low-level reflectivity from the value measured aloft:

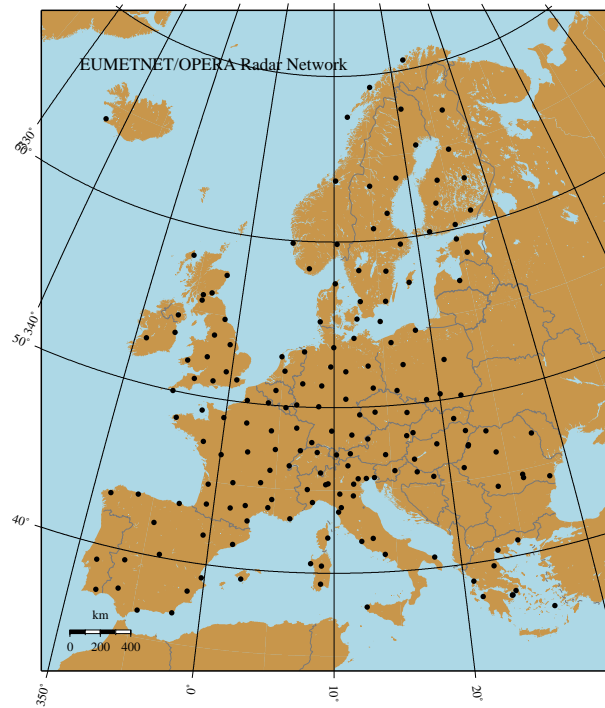


Figure 4: The OPERA radar network.

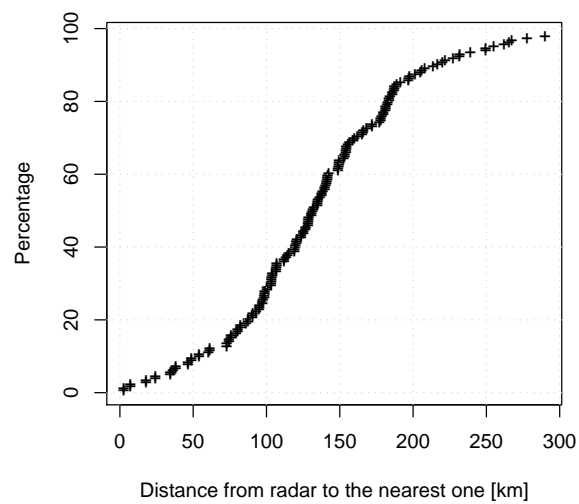


Figure 5: The percentage of radars as a function to the distance to the nearest radar. The data is based on entries at the OPERA database

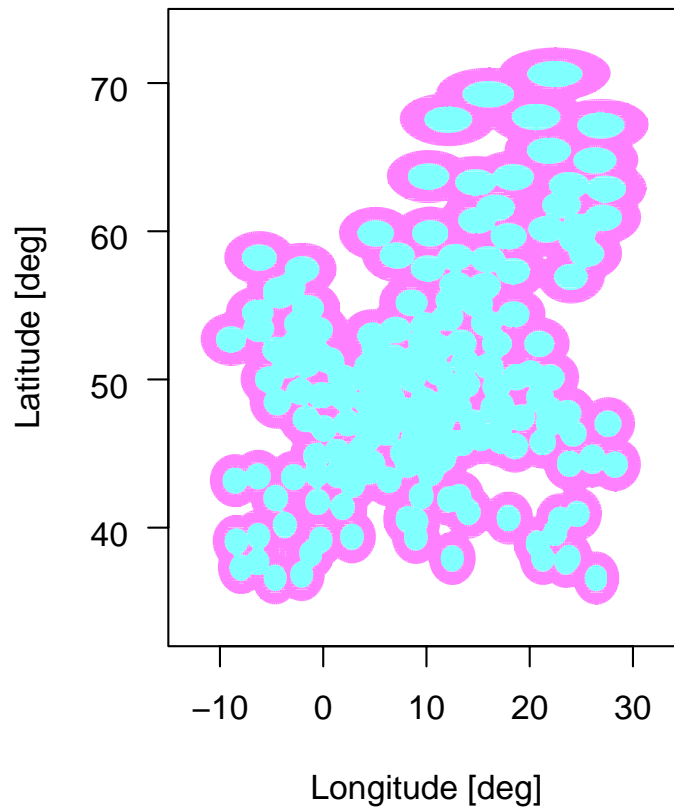


Figure 6: The distance to the closest radar. Locations with distance below 100 km are marked with cyan, and locations with distances from 100 to 200 km with magenta.

1. removal of non-meteorological echoes from the data (unless done during the volume data processing). Filling in gaps by using adjacent good quality data.
2. calculating the bending of the beam due to refraction to find out the altitude of the measurement as a function of range (we shall use standard refraction formulas here)
3. taking the attenuation due to hydrometeors into account
4. taking into account the difference of the altitude of the measurement and that of the product (profile correction)

### 5.3 Non-meteorological echoes, refraction and attenuation

The non-meteorological echoes and their treatment has been discussed in section 2.6. In the volume data processing the non wanted echoes have been removed, or a classification produced. Because the intended use of the low level reflectivity is to serve as a basis for precipitation products, only meteorological echoes are used when determining the low level reflectivity.

In case no valid data remains (in a pixel or larger area), various methods to estimate the data on the basis of adjacent good data is available. The most evident method is the interpolation from adjacent azimuths or elevations.

Radio waves, when travelling in the atmosphere, bend due to changes in the refractive index. In the usual case, where the refractive index decreases with increasing altitude, the wave bends downwards. Hence the altitude of the radar beam will be lower than the altitude calculated by the straight line propagation. A proper calculation requires that the refractive index  $n$ , which depends on the temperature, pressure and specific humidity, is known. If the gradient of  $n$  is constant, an analytic solution is obtained, and a typical gradient of  $-1/4R_E$  ( $R_E$  is the Earth radius) means that the altitude can be calculated assuming a straight line propagation, but with using a radius of  $4/3R_E$  in the calculation. This assumption is sufficient for most cases for altitude up to 10-20 km. (Doviak and Zrnić, 1993, chap. 2.2)

The attenuation due to hydrometeors, atmosphere, and wet radome has been discussed in section 2.7. According to the recommendation given, the atmospheric attenuation should be made to the volume data, but the attenuation correction due to hydrometeors should not, because the information needed is not available at that stage. To obtain fully correct low level reflectivities, and precipitation rates deduced thereof, the correction is needed. Care has to be exercised not to overestimate the attenuation and in that way to produce an error larger than that being corrected. According to Joss *et al.* (1998) it is extremely difficult to correct errors larger than around 2 dB two-way.

## 5.4 Correction of the effects of vertical displacement of radar measurements from the ground level

### 5.4.1 Introduction

The vertical profile of the radar reflectivity factor (VPR) and the measurement geometry of a weather radar introduce a difference between the reflectivity at the ground level and the radar measurement from the contributing volume aloft. Radar measurements are made at an increasing height and with an increasing measurement volume with an increasing range, making them decreasingly representative for the low level or ground conditions. A radar measurement ( $Z_e$ ), and possibly even a rainfall intensity or a snowfall intensity from the applied  $R(Z)$ -relation can be accurate aloft, at the height of radar measurement, but it is not necessarily valid at the surface of the earth. This inaccuracy is not a measurement error but a vertical sampling bias.

The sampling difference between the ground and the radar measurement aloft (S) can be corrected when the vertical profile of reflectivity factor (VPR) is known. Measured reflectivity factor  $Z_e(h, r)$  at a distance  $r$  and a height  $h$  from the surface is (Koistinen, 1991)

$$Z_e(h, r) = \int_{h_s(r)}^{H(r)} f^2(h(r) - y) Z_e(y) dy \quad (4)$$

where  $h_s$  is the upper edge of the shielding topography in the horizontal (azimuth) direction of the measurement,  $f$  the one way normalized beam pattern,  $H$  is an arbitrary height ( $H \gg h$ ) where  $f \rightarrow 0$ ,  $Z_e$  is the true vertical profile of reflectivity and  $y$  is the vertical co-ordinate. When we calculate the integral from Eq. 4, the vertical sampling difference  $S_h$  in dB units between the radar measurement at a height  $h$  and the reflectivity factor at the ground level  $h_g$  is obtained as

$$S_{h,r} = 10 \log \frac{Z_e(h_g, r)}{Z_e(h, r)} \quad (5)$$

where  $Z_e(h_g, r)$  is the reflectivity factor at the surface. The quantity  $S_{h,r}$  is often denoted as the vertical reflectivity profile correction.

In the history of the radar meteorology it has been understood relatively late that the difference between the radar estimate of the precipitation aloft and the in situ

measurement at ground is frequently the most significant bias in the radar based QPE in climates such as that in Europe (Zawadzki, 1984; Joss and Waldvogel, 1990). In the longer operational ranges of 100 - 250 km from radar the bias is often so large, 20-40 dB, that the reflectivity signal is lost completely and the real detection range of precipitation is only 100-150 km (Koistinen *et al.*, 2003). The same conclusion is valid also at shorter ranges, when mountains, hills or buildings introduce severe shielding for the low elevation beams (Germann and Joss, 2003). In this document we assume, on average, the distance to the nearest radar to be of the order of 100 km without severe shielding. In such relatively favorable measurement conditions the vertical sampling bias in most cases will be less than approximately 5 dB. Still in this range region the sampling difference can often be a much more important factor in the inaccuracy of low level reflectivity than any other source of error. Typical conditions when the bias is most significant, assuming that low level QPE is performed applying the lowest elevation PPI scan, are the following:

1. The bright band layer height is not more than approximately 1 km above the radar antenna. Then major part of the pulse volume can be located inside the melting layer introducing an overestimation of 2-8 dB. However, the overestimation is then restricted to a short, more or less circular range interval close to the radar (Smith, 1986, e.g.).
2. In a dry snowfall or in a very shallow winter time convective rain or in a drizzle the magnitude of the negative vertical reflectivity gradient is often several dB/km already within the lowest 2 km thick layer above the ground. Together with the possible occurrence of partial beam filling in the upper part of the precipitating layer it will introduce a significant and with the range increasing underestimation starting already at short distances from a radar Koistinen *et al.* (2003).
3. In a hilly or mountainous terrain the orographic enhancement of rainfall due to the low level growth of hydrometeors can be easily several dB below the lowest beam measurement (Germann and Joss, 2003).
4. Especially in the leading edge of widespread frontal precipitation bands and in areas of convective anvil clouds strong evaporation occur frequently. Evaporative conditions introduce much weaker reflectivity or even a complete evaporation of precipitation before the falling hydrometeors reach the ground level. The latter phenomenon is often called an overhanging or

elevated layer of precipitation (OP). For example in Finland 20 % of all precipitating VPRs are classified as OP (Koistinen *et al.*, 2003). In such conditions, typically at longer ranges (150-250 km) from radar, the lowest elevation beam can measure 5-30 dB higher values of reflectivity factor than actually could be detected at the ground level of the same vertical column.

Based e.g. on the yearly occurrence and climatology of VPRs measured at each radar site, the data operator can estimate the significance of each factor 1-4 in the list above. Quantitative evaluation can be performed applying Eq. 5 for all measured VPRs. Based on such knowledge one can decide on the periods and locations when such a correction is necessary. As a first guess, however, the authors feel that at least in winter a robust VPR correction should be performed always in the whole of Europe.

#### **5.4.2 Limitations of gauge-radar adjustment techniques to estimate low level precipitation**

In principle the sampling biases due to the fact that the vertical profile of reflectivity does not represent the ground level reflectivity, when radar based precipitation is still detectable, would be avoided by performing a gauge adjustment to radar data. As is shown e.g. by Michelson and Koistinen (2000) the radar bias due to VPR effects (in dBs) tends to be proportional to measurement range squared. However, removing the bias well with gauge-radar adjustment requires that the density of telemetering gauges must be high. An evaluation of radar-gauge merging methods and the impact of the gauge network density are presented in Goudenhoofdt and Delobbe (2009). In some countries, radar-gauge merging is the state of the art for 24h accumulations but not for shorter time periods. For example, in case of frontal passages the height and shape of VPRs and thus, the respective bias, can change dramatically during one day. Therefore an adjustment based on gauge-radar comparisons from the past can often fail in real time applications. Even when e.g. hourly gauge measurements could be available the short accumulation period tends to enhance random variation in gauge-radar comparisons making adjustments noisy. A further disadvantage in a gauge adjustment is that it is a "black box" method i.e. the adjustment factor may contain some permanent or transient, inseparable components of radar and gauge errors which can mask the sampling effects of the VPR and its proper correction. Also quite frequently the precipitating systems are located completely

or mostly between gauge locations. Therefore it is recommended to apply physically based real time VPR corrections to radar measurements for obtaining the optimal low level reflectivity.

Naturally such a practice does not exclude the benefits of applying also a gauge adjustment for longer periods e.g. for the purposes of removing possible calibration errors from the data (Holleman, 2007, e.g.). With calibration we denote here the electrical calibration of a radar system whereas the term adjustment denotes the correction of radar measurements with other measurements *in situ*. A gauge-radar discrepancy can contain calibration errors in both sensors, other errors and sampling differences. Thus gauge adjustment of radars may detect and remove major systematic electrical calibration errors (if gauge errors and sampling differences are small in relative terms) but can not replace an accurate radar calibration.

**Recommendation on profile correction:** It is recommended that a VPR correction is always performed to obtain a less biased low level reflectivity for the purposes of QPE.

### 5.4.3 Derivation and quality control of vertical reflectivity profiles from volume data

Several VPR correction schemes have been proposed and tested (Koistinen (1991), Kitchen *et al.* (1994), Joss and Lee (1995), Andrieu and Creutin (1995), Vignal *et al.* (2000), Marzano *et al.* (2002), Gray *et al.* (2003)). In principle they are all based on Eq. 5. The differences arise from the selected technique how the low level reflectivity is physically and mathematically estimated from the measured data aloft, possibly using assisting external data from NWP models or satellite measurements. The main difficulty is that the measurement geometry of a radar system, together with the shielding topography, prevents us from seeing the actual VPR at longer ranges above each geographical location at each moment in time. Hence we must estimate the profiles from either the measured high resolution volumetric data at close ranges to the radar or apply climatological reflectivity profiles.

Vertical profiles of reflectivity should be derived from the individual measured 3D polar volumes close to each radar, e.g. inside a range interval of 5-50 km. In such close distances it is possible to detect the vertical shape of the VPR with a

good resolution. A vertical resolution of 200 meters or better is recommendable to find out e.g. the thickness and amplitude of the bright band (if existing). The reflectivity value for each 200 meters thick layer can be obtained as a linear average of the radar reflectivity factor  $Z_e$  in those measurement bins where  $Z_e$  exceeds the noise level and where beam center is located within the selected layer.

In order to obtain physically realistic VPRs some quality control steps are recommended. In most cases, prior to layer averaging, the volume data has passed Doppler filtering to eliminate the effect of the ground clutter. As the filtering cannot reject fully the effect of the strongest clutter targets at short ranges to the radars, the measured VPR can still be enhanced by the clutter at the lowest layers. Quality control can be used to limit the vertical reflectivity gradient to be not steeper than e.g. -1 dB/200 m outside the melting layer. Additionally, each layer should contain enough measurement bins (e.g. at least 30 but preferably thousands) to be representative for it.

An additional quality operation can be applied to introduce vertical smoothing at higher altitudes so that reflectivity gradients between layers would not be physically unrealistic outside the bright band. A very essential issue in VPR corrections is the proper diagnosis of the height of the melting level. If polarimetric quantities are not available, a reliable method is to apply the vertical temperature information from very short range NWP fields, interpolated to time and place of the radar (Mittermeier and Illingworth, 2003). With such information it is rather easy to deduce which local maximum in a VPR is generated by the bright band (if found) and, consequently, which is the water phase of hydrometeors in the low or ground level reference value  $\text{dBZ}(h_g, r)$ . The latter defines the proper  $R(Z_e)$  conversion needed when low level reflectivity is transformed into precipitation intensity either in snow or in rain.

A further crucial aspect of the quality control of VPRs applying the height of melting level is the classification of the profiles into categories of scattering media. Migrating insects and birds as well as residual clutter introduce ground reaching VPRs which may resemble those of weak and shallow precipitation. Measured VPRs should be used for the derivation of the VPR-corrected low level reflectivity only if the profile applied represents that of precipitation. For example in Finland on average 40 % of all ground reaching VPRs are from clear air echoes or clutter. The classification can be based on the assumption that in the precipitation a moist adiabatic lapse rate of -6.5 °C/km prevails and the assumption that almost all the

precipitation in Europe is initiated in an ice crystal process in temperatures of  $-6$  °C or less (Rogers and Yau, 1989). This means that the top of the profile should be at least one kilometer above freezing level to be diagnosed as precipitation. All precipitation above the diagnosed bright band, based on the freezing level, is snow and liquid water below that. The assumption implies also that we are not able to diagnose shallow drizzle or other coalescence driven rain from clear air echo or clutter.

#### 5.4.4 Integration in time and place and limitations

The magnitude of the correction factor ( $S$ ) in creating the low level reflectivity at longer ranges is quite sensitive to variations in the vertical shape of the VPR in time and space. The 50 km range inside which the VPR is derived represents typically less than 10 % of the coverage area of a single radar. In order to avoid spurious transient reflectivity corrections in the whole coverage area, integration in time and in space is needed. The measured profiles themselves should not be integrated in time as the resulting average profile can easily become physically unrealistic (e.g. the average bright band can become very thick if the height of the melting level is rapidly changing). It is recommended to derive an ensemble of VPR corrections at each location inside a time window which represents the length of the period when a VPR moves across the radar measurement area. The length of such a time window is some 6 hours if we assume a velocity of 10 m/s for the precipitating weather system. The ensemble members are obtained by applying independently each profile measured during the time window. The final, and hopefully the best average VPR correction at each location is then the average of the ensemble of corrections.

The periods when the precipitation is detected but does not occur widely enough inside the range belt of the VPR derivation are frequent. A convenient way is to apply climatologic VPRs at those time moments. A simple profile consists typically of fixed vertical reflectivity gradients below and above the bright band as well as a bright band whose thickness and amplitude (in dBs) are obtained by studying a representative and large sample of measured VPRs. Very important is that the climatologic profile is not fixed in altitude but moves up and down in real time based on the estimated freezing level height obtained from very short range NWP fields, interpolated to the moment of radar measurement. It has been shown that such climatologic VPRs remove the major part of the sampling

bias and produce good estimates of low level reflectivity (Koistinen (1991), Joss and Lee (1995)). Thus a climatologic VPR correction is a kind of recommendable minimum solution for the production of operational low level reflectivity.

When both climatological VPR correction and that based on actual volumes (from the correction ensembles) are available simultaneously it is recommended to derive the final, operational low level reflectivity by applying a weighted average of the two. The relative weight can vary in time so that in cases of high quality measured VPRs the relative weight of the climatologic profile is small.

A further problem appears when we try to apply VPR corrections in a radar network. Although straightforward with a single radar system, slightly different VPR corrections, applied independently at neighboring radars, easily amplify reflectivity discrepancies where data from two neighboring radars meet in a radar network composite product. At each network composite pixel the magnitude of the VPR correction is a weighted mean of the corrections derived at each radar site at the range where the location is seen from the two radars. The weights can be determined e.g. inversely proportional to the distance. It should be noted that with weighted correction from two radars we can still use measured reflectivity from one radar only (usually the closest one).

If the VPR correction is very large (shallow precipitation at longer ranges) or the uncorrected dBZ is already quite high, the magnitude of the correction should be limited to avoid unrealistically high precipitation intensities e.g. in cases of embedded convection. For example in Finland the upper limit of any VPR correction is 30 dB together with a scheme which allows less and less small positive increments to the measured reflectivity when it increases from 50 to 70 dBZ.

Layers of elevated precipitation (OP), not reaching the ground, or areas of quite significant evaporation are problematic for any correction based on an observed VPR close to a radar. Actually the correction factor to obtain low level reflectivity in areas of OP is the measured dBZ with a minus sign i.e. removal of the measured reflectivity. As the diagnosis of areas of overhanging precipitation is quite difficult in long ranges from radar, no robust method has been so far invented to detect and remove elevated layers of reflectivity in the products supposed to represent ground or close to ground level. In parallel, layers of strong evaporation in the measured VPRs can be a risk for hydrology as they introduce large negative VPR corrections. It is possible that evaporation occurs close to a radar in conjunction with decaying or weak weather systems but not necessarily at longer range where

a severe storm can still be located simultaneously.

## 5.5 Requirements on volume data

General aspects of volume data have been discussed already in Section 2. Although in practice volume scan characteristics are a compromise between many influencing factors and competing interests the best estimate of the low level reflectivity is obtained with appropriate scanning strategies and system properties, summarized in the following:

1. The antenna should be located in a place where minimal beam blocking exists at least close to the radar (approximately 30-60 km) for measuring the shape of VPR. On the other hand, the lowest elevation beam should be as close to the ground level as possible, in order to be able to detect at least in most rainfall cases reflectivities below the bright band. Although it is possible to estimate VPR corrections based only on two elevation angles (Smith 1986) a high resolution VPR at close ranges can be obtained best by applying roughly 10 or more elevation angles. In order to obtain many samples of VPRs in time, representing better the whole radar coverage area, it is recommended to perform a full volume scan at least every 30 minutes.
2. The reflectivity data should pass a high quality Doppler filtering, or some other efficient methods of clutter removal. Otherwise the VPRs obtained may contain residual clutter at low elevation angles leading easily to too steep negative vertical reflectivity gradients and, thus, to too large VPR corrections in estimations of low altitude reflectivity.
3. Radar systems equipped with polarization diversity are recommended for diagnosing VPRs or those parts of VPRs generated by non-meteorological scatterers and for diagnosing the height of the melting layer. The latter can be also obtained rather well if a Doppler measurement is performed using vertically pointing antenna. However, a vertically pointing scan is not sufficient for obtaining a good VPR itself as the number of reflectivity samples (bins) in each vertical layer is not representative enough.

## 6 Note on the frequency band and on the use of dual-polarization

### 6.1 Choice of the frequency band

The discussion above has been made with the C-band in mind. At some places where the choice of the frequency has its effect, the difference between the C-band and the S-band has been briefly discussed. In summary, for the following reasons it would be of beneficial to choose S-band:

1. Attenuation due to hydrometeors is significantly smaller in S-band, and can be neglected. This improves the quality of the reflectivity and rain rate estimates at longer ranges.
2. The range-Doppler dilemma is less severe by a factor of 2. Hence it is easier to produce wind data for high limiting velocities.
3. There are fewer sources of radio frequency interference at S-band, which increases the quality of observations.

However, this is obtained with the following cost:

1. To achieve the same beam width, an antenna with doubled size is needed. This is more costly, and also increases the cost of the radar tower. Some other hardware components are also more expensive, which increases the cost.
2. The scattered power is proportional to  $\lambda^{-4}$ , and hence the sensitivity at the S-band is lower by a factor of 16. This can be partly compensated by using a higher transmitted power, which in turn increases the cost.

Hence we can summarize that S-band offers a better way to obtain high quality reflectivity data, and precise quantitative precipitation estimates, as well as high quality wind data. This is obtained by an increased cost and loss of sensitivity.

### 6.2 Dual polarization

The use of the dual-polarization will surely change the way radar measurement are carried out, and products calculated, and will increase the number of products.

The work to assess the effects is ongoing in parallel to this work (Tabary *et al.*, 2009). At present there is still not much experience of the operational use of dual-polarization, but the technique has a great potential due to the following benefits (these appear in the order the items are discussed in this document):

1. A great number of new products are available for the classification of echoes, and to separate meteorological and non-meteorological echoes. This will increase the quality of the data, as well as provide new products (e.g. hydrometeor phase).
2. The detection and removal of the ground clutter will be more efficient.
3. Dual-polarization moments provide data on the attenuation, which will improve the quantitative precipitation estimates at C-band.

## 7 Appendices

### A Finite bandwidth loss and the effective pulse length

The received power of a radar depends on the pulse length. Although the nominal pulse length appears in the radar equation, the received power is slightly smaller, because the impulse response of the receiver has its effect on the power. This means that the effective pulse length is smaller than the nominal one. Another way to describe this is to consider this as a loss in the receiver filtering. This effect is well-known and described in standard text books (Doviak and Zrnić, 1993, chap. 4.4.3). In the following we use the formalism presented by Lehtinen and Huuskonen (1996).

Let  $env$  be the envelope of the transmitted pulse and  $p$  the receiver impulse response. Assume further that

$$\int p(t)dt = 1 \tag{6}$$

Then the receiver bandwidth is

$$\int p^2(t)dt \tag{7}$$

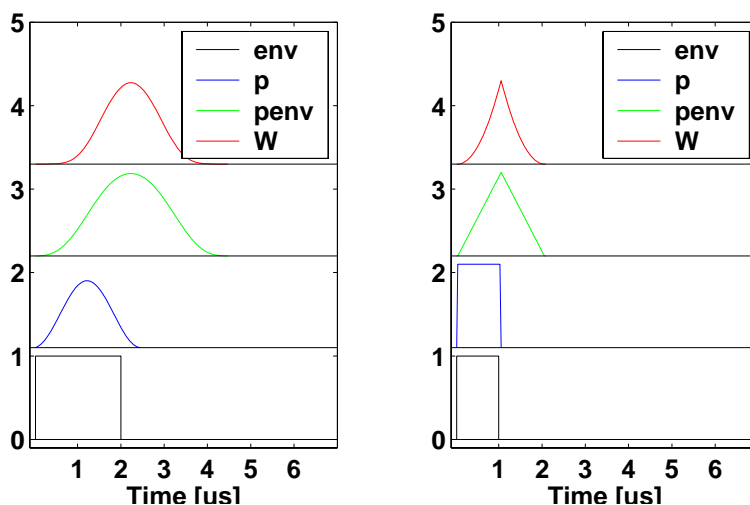


Figure 7: The transmitter envelope (*env*), filter impulse response (*p*), effective pulse form (*penv*) and the range weighting function (*W*) using a realistic impulse response (left) and a box-car impulse response (right)

The convolution of *p* and *env* gives the effective pulse form *penv* (as seen by the receiver)

$$\text{penv} = p * \text{env} = \int p(\tau)\text{env}(t - \tau)d\tau \quad (8)$$

The range weighting function *W* is the square of *penv*. As the latter may be complex we write

$$W(t) = \text{penv}(t)\overline{\text{penv}(t)} \quad (9)$$

The effective pulse length is then the integral of *W*

$$l = \int W(t)dt \quad (10)$$

and the finite bandwidth loss is the effective length divided by the nominal length  $l_{nom}$

$$\frac{l}{l_{nom}} \quad (11)$$

For a square pulse, and a receiver with an square impulse response the loss is 1.7 dB. This is easily seen. The convolution of a square pulse of unit height and length with an impulse response of unit height and length is a triangle of two units long and height one. Squaring gives two parabolic functions, the area under which is  $2/3$  (the effective pulse length). This equals to 1.7 dB. This is portrayed in Fig. 7. For the FMI Luosto radar the value is 1.3 dB, calculated with real

pulse forms and impulse responses. Doviak and Zrnić (1993) give a value of 1.8 dB for a Gaussian filter shape and 2.3 dB for a practical matcher filter.

The finite bandwidth loss is unavoidable, because a properly designed receiver has a bandwidth which is matched to the transmitted pulse so that the SNR is maximized. A wider receiver bandwidth would pass more signal power through, but at the expense of increasing the noise power, and a narrower receiver bandwidth would limit the noise power at the expense of reducing the signal power.

If the calibration injection is pulsed, the loss is taken into account automatically in the calibration process. Otherwise it has to be included in one of the calibration constants.

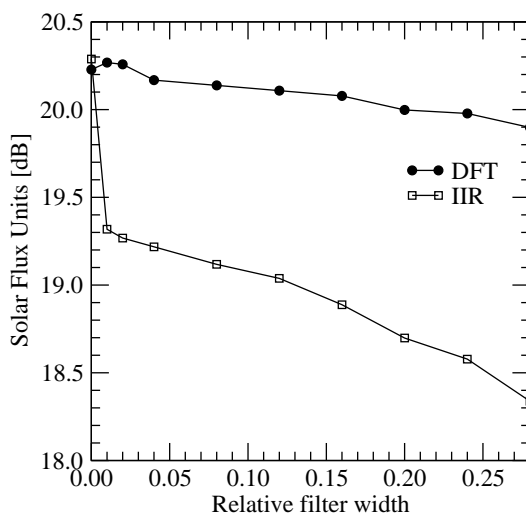


Figure 8: Received solar flux as a function of the width of the Doppler clutter filter relative to the unambiguous velocity. Curves for both frequency-domain (DFT) and time-domain (IIR) filters are shown. Data are obtained during offline sun tracking in De Bilt on 9 July 2008. Figure courtesy of Iwan Holleman, KNMI.

## B Power loss caused by the Doppler filtering

The high pass filtering of the radar raw data, which is implemented in the signal processing to remove the ground clutter, also removes some parts of the weather signal. There is no way for the time domain high pass filter to know whether a frequency component close to the zero frequency is caused by reflections from the ground or from drops with zero radial velocity. The outcome of this is the infamous "Doppler snake" which is seen as a reduced Z value along the zero

velocity line. The line is often curved, hence the name.

Recent studies on using the sun signal to monitor the received power (Holleman *et al.*, 2009) have indicated that the high pass filters implemented in radar signal processors actually can have a significant attenuation also off the stop band of the filter. Figure 8 shows the attenuation of the sun signal as a function of the filter width for a time-domain (IIR) filter and for a frequency-domain (DFT) filter, as implemented in the Dutch weather radar network.

As the plot is made for sun signal, which is a wide band noise like signal, and not a narrow band weather signal, some interpretation of the figure is essential to reach the conclusions. The curve for the IIR-filter shows a sharp drop when even the narrowest filter is applied, and then a gradual decrease with an increasing filter width. This gradual decrease is in agreement with the increasing width, and confirms that more sun power is filtered out with a wider filter. The effect on the weather signal depends on the radial velocity component. If it is within the stop band, the Doppler snake effect is seen, and if outside, no influence or a small influence is visible. The drop from the zero width to the narrowest filter indicates that the filter has a non-zero attenuation all along the pass band, amounting to roughly 1 dB. This attenuation affects the sun and weather signal alike. Hence all weather signal are attenuation at least by 1 dB, and even more if the radial velocity is within the stop band of the filter.

The frequency domain DFT-filter has similar characteristics as a function of the filter width, but the sharp decrease at the zero width is missing. Hence we conclude that this filter will not produce an overall attenuation of the weather signal. The attenuation in the case the radial velocity is within the stop band of the filter cannot be determined by using these data.

## References

- Andrieu, H. and J. D. Creutin, 1995: Identification of vertical profiles of reflectivity for hydrological application using an inverse method: Part I: formulation. *J. Appl. Meteorol.*, **34**, 225–239.
- Chèze, J.-L., S. Hafner, I. Holleman, S. Matthews, and D. Michelsen, 2009: Specification of the EUMETNET operational weather radar data center. OPERA deliverable OPERA/2008/02, EUMETNET OPERA, 33 pp.
- Divjak, M., P. L. Berre, D. Bižić, C. Ciotti, M. R. Dias, G. Galli, A. Huuskonen, D. Kotlarikova, J. Kračmar, J. Nagy, K.-J. Schreiber, and W. K. Wheeler, 1999: Radar data quality-ensuring procedures at European weather radar stations. OPERA deliverable WD/09/1999, EUMETNET OPERA, 12 pp.
- Doviak, R. J. and D. S. Zrnić, 1993: *Doppler Radar and Weather Observations*, Second edition. Academic Press, 562 pp.
- Germann, U. and G. Galli, 2003: Recommendations for radar data acquisition procedures. OPERA deliverable WD/05/2003, EUMETNET OPERA, 9 pp.
- Germann, U. and J. Joss, 2003: Operational measurement of precipitation in mountainous terrain. *Weather Radar: Principles and Advanced Applications*, P. Meischner, ed., Springer, Berlin Heidelberg, 52–77, ISSN 1610-1677, ISBN 3-540-000328-2.
- Goudenhoofdt, E. and L. Delobbe, 2009: Evaluation of radar-gauge merging methods for quantitative precipitation estimates. *Hydrol. and Earth Syst. Sci.*, **13**, 195–203.
- Gray, W. R., M. J. Uddstrom, and H. R. Larsen, 2003: Radar surface rainfall estimates using a typical-shape function approach to correct for the variations in the vertical profile of reflectivity. *Int. J. Remote Sensing*, **23**, 2489–2504.
- Holleman, I., 2003: Doppler radar wind profiles. Scientific report, KNMI WR-2003-02, KNMI, 72 pp.
- 2005: Quality control and verification of weather radar wind profiles. *J. Atmos. oceanic Techn.*, **22**, 1541–1550.
- 2007: Bias adjustment and long-term verification of radar based precipitation estimates. *Meteorol. Applications*, **14**, 195–203.

- Holleman, I. and H. Beekhuis, 2003: Analysis and correction of dual PRF velocity data. *J. atmos. oceanic Techn.*, **20**, 443–453.
- Holleman, I., A. Huuskonen, M. Kurri, and H. Beekhuis, 2009: Monitoring of weather radar receivers using solar signals detected in operational scan data. *J. atmos. oceanic Techn.*, in press.
- Holleman, I., D. Michelson, G. Galli, U. Germann, and M. Peura, 2006: Quality information for radars and radar data. OPERA deliverable OPERA/2005/19, EUMETNET OPERA, 77 pp.
- Holleman, I., H. van Gasteren, and W. Bouten, 2008: Quality assessment of weather radar wind profiles during bird migration. *J. atmos. oceanic Techn.*, **25**, 2188–2198.
- Huuskonen, A. and I. Holleman, 2007: Determining weather radar antenna pointing using signals detected from the sun at low antenna elevations. *J. atmos. oceanic Techn.*, **24**, 476–483.
- Joss, J. and R. Lee, 1995: The application of radar-gauge comparisons to operational precipitation profile corrections. *Appl. Meteorol.*, **34**, 2612–2630.
- Joss, J., B. Schädler, G. Galli, R. Cavalli, M. Boscacci, E. Held, G. Bruna, G. Kappenberger, V. Nespor, and R. Spiess, 1998: Operational use of radar for precipitation measurements in Switzerland. Final report, NRP31, ETH Zürich, 108 pp.
- Joss, J. and A. Waldvogel, 1990: Precipitation measurements and hydrology. *Radar in meteorology*, D. Atlas, ed., AMS, Boston, 577–606.
- Kitchen, M., R. Brown, and A. G. Davies, 1994: Real-time correction of weather radar data for the effects of bright band, range, and orographic growth in widespread precipitation. *Quart. J. Roy. Meteorol. Soc.*, **120**, 1231–1254.
- Koistinen, J., 1991: Operational correction of radar rainfall errors due to vertical reflectivity profile. *25th Conference on Radar Meteorology*, AMS, 91–94.
- Koistinen, J., D. B. Michelson, H. Hohti, and M. Peura, 2003: Operational measurement of precipitation in cold climates. *Weather Radar: Principles and Advanced Applications*, P. Meischner, ed., Springer, Berlin Heidelberg, 78–114, ISSN 1610-1677, ISBN 3-540-000328-2.

- Kurri, M. and A. Huuskonen, 2008: Measurements of the transmission loss of a radome at different rain intensities. *J. atmos. oceanic Techn.*, **25**, 1590–1599.
- Lehtinen, M. S. and A. Huuskonen, 1996: General incoherent scatter analysis and GUISDAP. *J. atmos. terr. Phys.*, **58**, 435–452.
- Manz, A., L. Handwerker, M. Löffler-Mang, R. Hannesen, and H. Gysi, 1999: Radome influence on weather radar system with emphasis to rain effects. *29th Conference on Radar Meteorology*, AMS, 918–921.
- Marzano, F. S., E. Picciotti, and G. Vulpiani, 2002: Reconstruction of rainrate fields in complex orography from C-band volume data. *Second European Conference on Radar Meteorology*, Copernicus Gesellschaft, 227–232.
- Meischner, P., ed., 2003: *Weather radar, principles and advanced applications*. Springer, Berlin Heidelberg, 337 pp., ISSN 1610-1677, ISBN 3-540-000328-2.
- Michelson, D. B. and J. Koistinen, 2000: Gauge-radar network adjustment for the baltic sea experiment. *Phys. Chem. Earth (B)*, **25**, 915–921.
- Mittermeier, M. P. and A. J. Illingworth, 2003: Comparison of model-derived and radar-observed freezing-level heights: Implications for vertical reflectivity profile correction scheme. *Quart. J. Roy. Meteorol. Soc.*, **129**, 83–96.
- OPERA, 1999: Timestamps in radar products. OPERA working document WD/16/99, EUMETNET OPERA, 1 pp.
- Peura, M., 2002: Computer vision methods for anomaly removal. *Second European Conference on Radar Meteorology*, Copernicus Gesellschaft, 312–217.
- Pohjola, H. and U. Gjertsen, 2006: Use of radar data by operational user communities. OPERA deliverable OPERA/2005/17, EUMETNET OPERA, 52 pp.
- Rogers, R. R. and M. K. Yau, 1989: *A Short Course in Cloud Physics*, Third edition. Butterworth Heinemann, 293 pp.
- Saltikoff, E. and I. Holleman, 2004: Recommendations for optimal settings to produce good quality wind soundings (vvp and vad) in operational radar networks. OPERA working document WD/2004/14, EUMETNET OPERA, 13 pp.

- Smith, C. J., 1986: The reduction of errors caused by bright bands in quantitative rainfall measurements made using radar. *J. Atmos. Oceanic Techn.*, **3**, 129–141.
- Tabary, P., M. Frech, and P. Dempsey, 2009: Opera III work package 1.4a, Evaluation of new technologies. OPERA deliverable OPERA/2009/02, EUMETNET OPERA, 106 pp.
- Vignal, B., G. Galli, J. Joss, and U. Germann, 2000: Three methods to determine profiles of reflectivity from volumetric radar data to correct precipitation estimates. *J. Appl. Meteorol.*, **39**, 1715–1726.
- WMO, 2006: *Guide to Meteorological Instruments and Methods of Observation*, No. 8, Seventh edition. Secretariat WMO, Geneva, Switzerland.
- Zawadzki, I., 1984: Factors affecting the precision of radar measurements of rain. *22nd Conference on Radar Meteorology*, AMS, 251–256.